**Supporting Information**

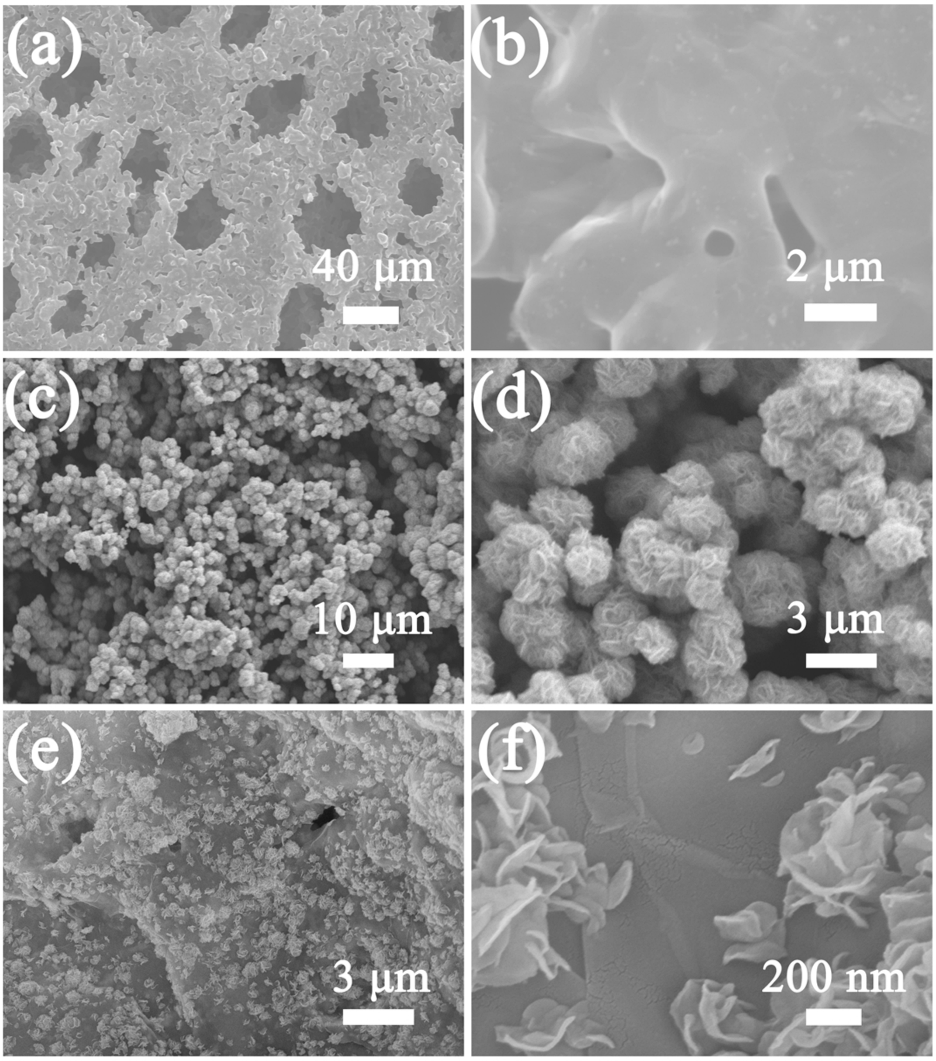


**Fig. S1.** FESEM images of (a, b) NPG and NPG@$WS_2$ prepared at (c, d) high and (e, f) low concentrations.

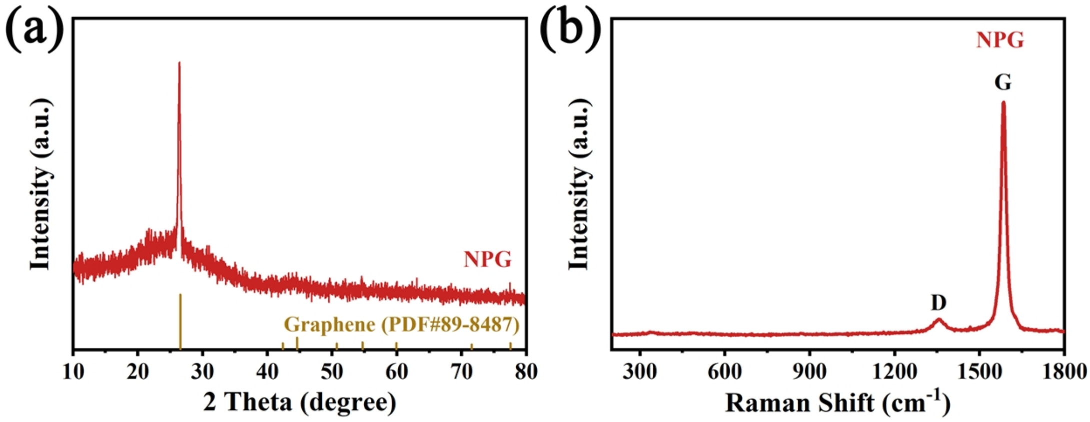


**Fig. S2.** (a) XRD patterns and (b) Raman spectra of NPG.

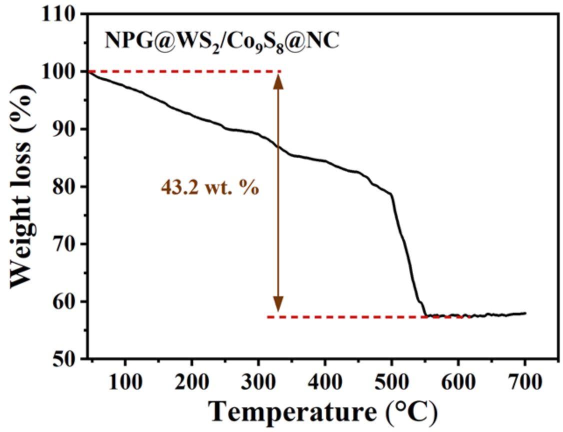


**Fig. S3.** TG analysis of NPG@$WS_2$/$Co_9S_8$@NC.

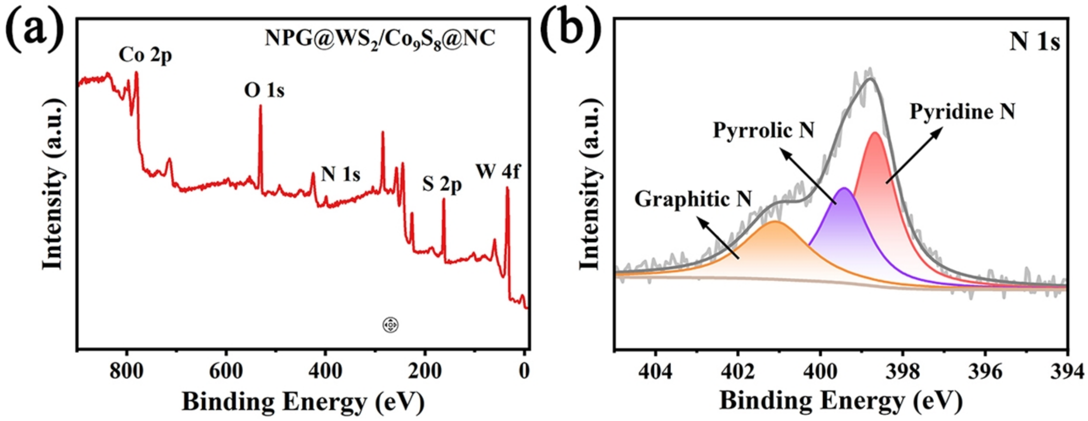


**Fig. S4.** XPS analysis of (a) NPG@$WS_2$/$Co_9S_8$@NC and (b) high-resolution N 1s.

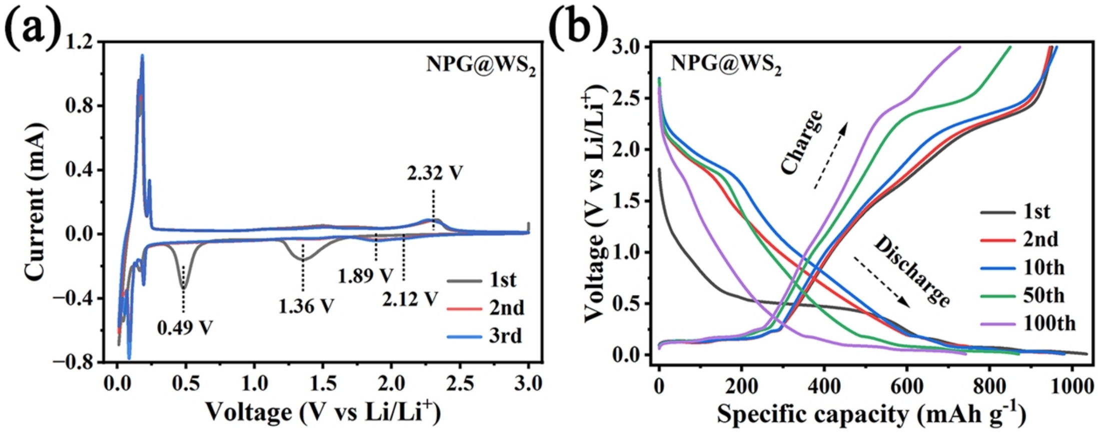


**Fig. S5.** (a) The initial three CV curves at a scan rate of 0.1 mV $s^{-1}$ and (b) the 1st, 2nd, 10th, 50th and 100th galvanostatic discharge/charge curves of NPG@$WS_2$ as anode for LIB within a voltage window of 0.01-3.0 V at a current density of 500 mA $g^{-1}$.

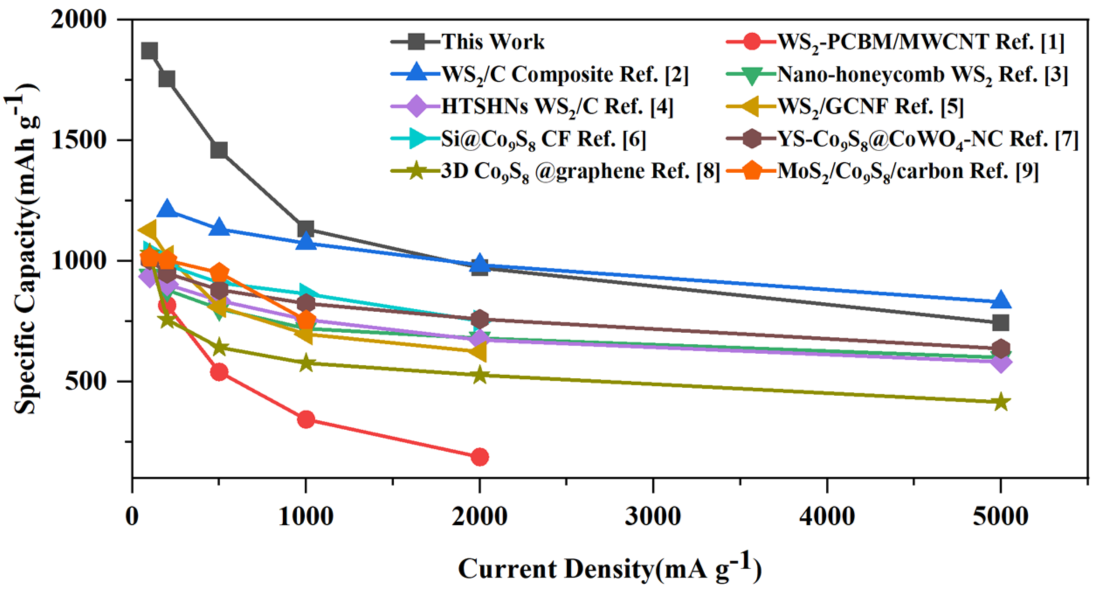


**Fig. S6.** Comparison of rate capability for LIBs between NPG@$WS_2$/$Co_9S_8$@NC and $WS_2$-based (or $Co_9S_8$-based) anodes reported in the recent literatures.

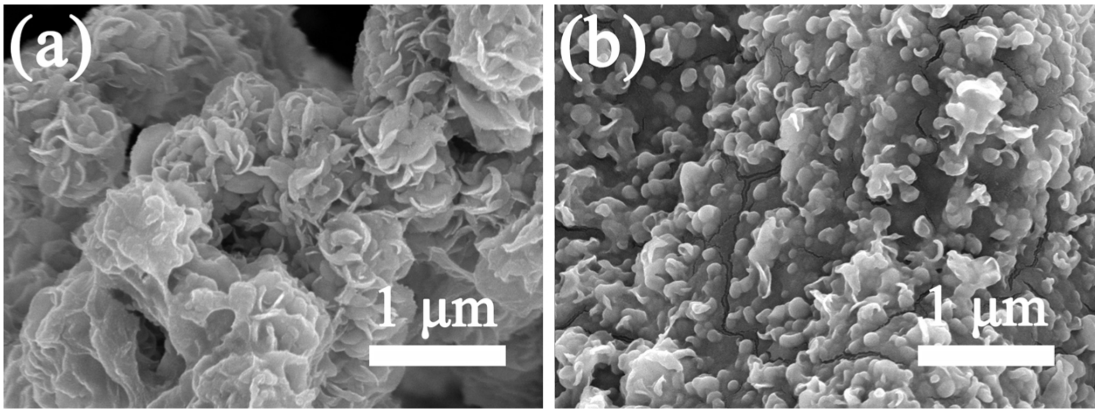


**Fig. S7.** SEM images of (a) NPG@$WS_2$/$Co_9S_8$@NC and (b) NPG@$WS_2$ materials after 200 cycles at 0.5 A $g^{-1}$.

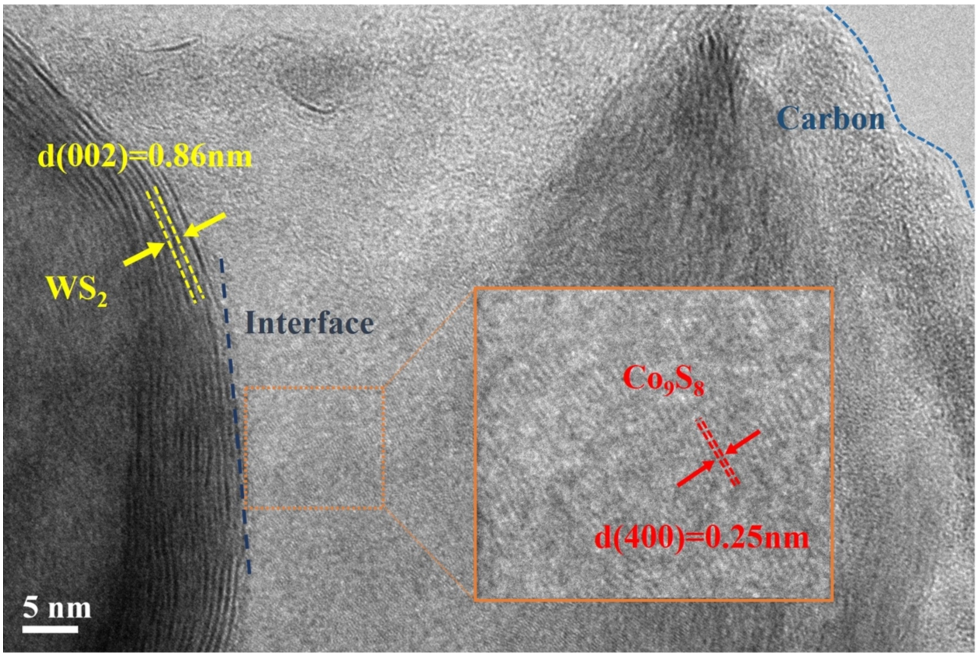


**Fig. S8.** HRTEM image of NPG@$WS_2$/$Co_9S_8$@NC materials after 200 cycles at 0.5 A $g^{-1}$.

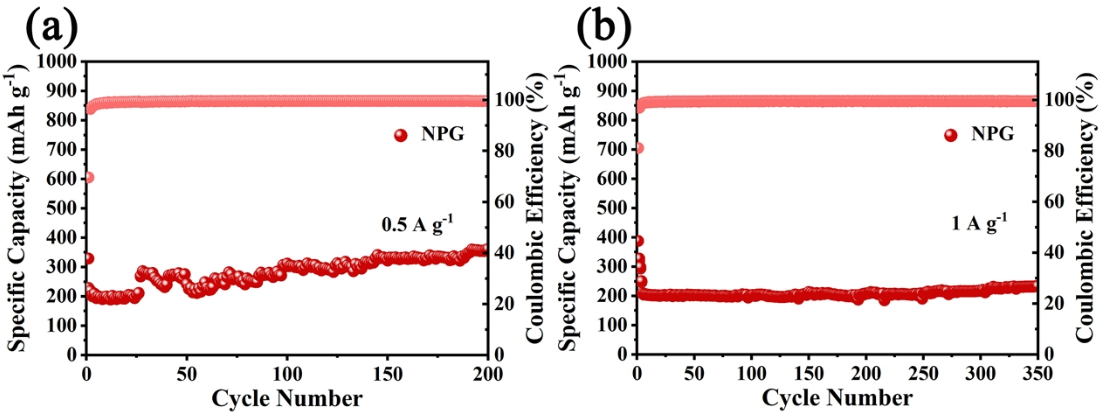


**Fig. S9.** Cycling performance and Coulombic efficiency of NPG at (a) 0.5 A $g^{-1}$ and (b) 1 A $g^{-1}$

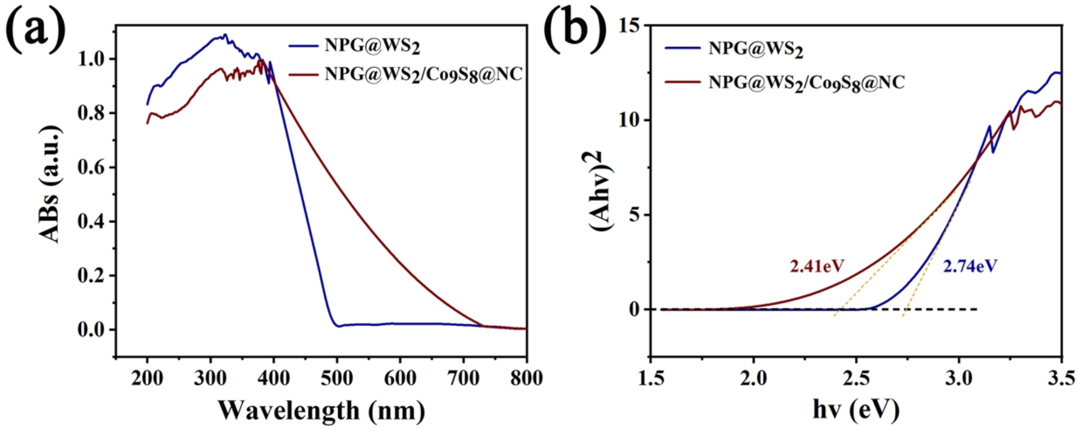


**Fig. S10.** (a) UV-vis DRS spectra and (b) Tauc plots of NPG@$WS_2$ and NPG@$WS_2$/$Co_9S_8$@NC.

**Table S1.** Comparison of cycling performance for LIBs between NPG@$WS_2$/$Co_9S_8$@NC and $WS_2$-based (or $Co_9S_8$-based) anodes reported in the recent literatures.

| Materials | Current density (mA $g^{-1}$) | Cycles | Capacity (mAh $g^{-1}$) | Ref. |
|---|---|---|---|---|
| $WS_2$-PCBM/MWCNT | 500 | 50 | 655.47 | 1 |
| $WS_2$/C Composite | 500 | 1000 | 1166.8 | 2 |
| Nano-honeycomb $WS_2$ | 1000 | 300 | 800 | 3 |
| HTSHNs $WS_2$/C | 1000 | 1000 | 784 | 4 |
| $WS_2$/GCNF | 100 | 100 | 1068.5 | 5 |
| Si@$Co_9S_8$ CF | 1000 | 250 | 633.6 | 6 |
| YS-$Co_9S_8$@$CoWO_4$-NC | 500 | 100 | 1053 | 7 |
| 3D $Co_9S_8$ @graphene | 1000 | 1000 | 550 | 8 |
| $MoS_2$/$Co_9S_8$/carbon | 200 | 50 | 987.7 | 9 |
| NPG@$WS_2$/$Co_9S_8$@NC | 500 | 200 | 1896 | This work |

**Table S2.** EIS specific descriptions of NPG@$WS_2$ and NPG@$WS_2$/$Co_9S_8$@NC electrode at various states.

| Samples | Rs (Ω) | Rct (Ω) |
|---|---|---|
| NPG@$WS_2$/$Co_9S_8$@NC after 10 cycles | 1.59 | 162.5 |
| Fresh NPG@$WS_2$/$Co_9S_8$@NC | 2.91 | 489.8 |
| NPG@$WS_2$ | 16.52 | 679.5 |

**References**

1. B. Mondal, A. Azam and S. Ahmad, PCBM Functionalized $WS_2$ Hybrid Nanostructures for High Performance Li-Ion Battery Anodes: Toward Binder-Free Electrodes, *Energy Fuels*, 2023, **37**, 16105-16118.
2. Z. W. Li, F. Yuan, M. S. Han and J. Yu, Atomic-Scale Laminated Structure of O-Doped $WS_2$ and Carbon Layers with Highly Enhanced Ion Transfer for Fast-Charging Lithium-Ion Batteries, *Small*, 2022, **18**, 2202495.
3. Y. C. Song, J. X. Liao, C. Chen, J. Yang, J. C. Chen, F. Gong, S. Z. Wang, Z. Q. Xu and M. Q. Wu, Controllable morphologies and electrochemical performances of self-assembled nano-honeycomb $WS_2$ anodes modified by graphene doping for lithium and sodium ion batteries, *Carbon*, 2019, **142**, 697-706.
4. X. E. Zhang, R. F. Zhao, Q. H. Wu, W. L. Li, C. Shen, L. B. Ni, H. Yan, G. W. Diao and M. Chen, Ultrathin $WS_2$ nanosheets vertically embedded in a hollow mesoporous carbon framework - a triple-shell structure with enhanced lithium storage and electrocatalytic properties, *J. Mater. Chem. A*, 2018, **6**, 19004-19012.
5. L. S. Zhang, W. Fan and T. X. Liu, Flexible hierarchical membranes of $WS_2$ nanosheets grown on graphene-wrapped electrospun carbon nanofibers as advanced anodes for highly reversible lithium storage, *Nanoscale*, 2016, **8**, 16387-16394.
6. X. P. Du, Y. Huang, Z. H. Feng, X. P. Han, J. M. Wang and X. Sun, Encapsulating yolk-shelled Si@$Co_9S_8$ particles in carbon fibers to construct a free-standing anode for lithium-ion batteries, *Appl. Surf. Sci.*, 2023, **610**, 155491.
7. Y. Zheng, Y. Xu, J. P. Guo, J. D. Li, J. J. Shen, Y. Guo, X. Z. Bao, Y. K. Huang, Q. Zhang, J. C. Xu, J. Wu, H. Ian and H. Y. Shao, Cobalt sulfide nanoparticles restricted in 3D hollow cobalt tungstate nitrogen-doped carbon frameworks incubating stable interfaces for Li-ion storage, *Electrochim. Acta*, 2022, **431**, 141134.
8. S. Y. Xu, X. C. Cao, F. Li, H. Li, H. Y. Qi, J. Zhang, C. Y. Chen and D. C. Ju, Novel 3D $Co_9S_8$@graphene nanocomposites prepared by deep eutectic solvents for lithium-ion storage, *J. Alloys Compd.*, 2023, **936**, 168080.
9. B. Wu, R. Ma, X. W. Liu, Y. Q. Zheng, S. S. Guo, Y. M. Yi, M. T. Sun, S. H. Wang and T. Wen, Self-assembly synthesis of petal-like $MoS_2$/$Co_9S_8$/carbon nanohybrids for enhanced lithium storage performance, *Front. Energy Res.*, 2022, **10**, 918494.